Sampling Based Multi-User Detector for Uplink Massive MIMO Communication Networks

Gopal Chamarthi[‡], Adarsh Patel[‡], Rameshwar Pratap[♮]
[‡]School of Computing and Electrical Engineering (SCEE), Indian Institute of Technology Mandi, Mandi, India
[♮]Department of Computer Science Engineering, Indian Institute of Technology Hyderabad, Hyderabad, India
Email: UD22010@students.iitmandi.ac.in, adarsh@iitmandi.ac.in, rameshwar@cse.iith.ac.in

***Abstract*—Massive multiple-input multiple-output (MIMO) systems are vital to current-generation wireless networks and provide reliable communication at higher data rates. This advantage comes at the cost of enhanced signal processing at the receiver. This work proposes a novel rescaled Kronecker volume sampling (RKVS) based efficient multi-user data detector for uplink massive MIMO communication networks. The proposed RKVS detector has a faster asymptotic run-time than linear detectors like zero-forcing (ZF), minimum mean squared error (MMSE), and low-complexity approximations having polynomial run-time complexity. Theoretical analysis shows that the RKVS detector's test statistic is an unbiased estimator of the ZF detector's test statistic. Numerical results further prove that the error performance of the RKVS detector lies in close approximation to the ZF detector and is superior to detectors employing state-of-the-art sampling-based regression approximation.**

***Index Terms*—Massive MIMO, multi-user detector (MUD), Sampling, Kronecker Regression.**

I. Introduction

The advent of 5G communication networks [1] caters to bandwidth-hungry user applications like 4K video streaming, extended reality, cloud computing, etc. Extensive deployment of Internet of Things devices alongside broadband and mobile users in 5G communication networks has led to a huge number of connected devices [1], with the current monthly global mobile network data traffic topping 145 exabytes [2].

The massive multiple-input multiple-output (MIMO) technology is a key enabler in 5G communication networks, providing an ever-increasing number of users with reliable connectivity at high data rates [3]. Massive MIMO systems allow users to utilize time-frequency resources, ensuring efficient resource utilization simultaneously. Similarly, extremely large (XL) MIMO systems employ thousands of base station (BS) antennas to provide massive, reliable access with high spectral and energy efficiency in beyond 5G networks [4]. However, efficiency in resource utilization in massive/ XL-MIMO systems comes at the cost of high signal processing complexity [4], [5].

Consider the signal detection problem in an uplink massive MIMO scenario with M antennas at the BS serving U single antenna users. Linear detectors like zero forcing (ZF) and minimum mean-squared error (MMSE) with asymptotic run-time complexity of $O(MU^2)$ are preferred over optimal maximum likelihood (ML) detector with an exponential run-time complexity, and other non-linear detectors [6]. The large number of BS antennas in massive MIMO systems makes even the linear detectors to be computationally intensive. Low-complexity linear detectors for massive MIMO communication networks have been developed recently [5], [7]. The existing low-complexity alternatives to ZF and MMSE detectors reduce complexity by approximating the matrix inversion with series-based approximations, like Neuman series-based matrix inversion approximation (NS-MIA) [8], Truncated polynomial expansion (TPE) [9], etc., or iterative method based approximations like Gauss-Seidel (GS) [10], successive over-relaxation (SOR) [11], Richardson iteration [12], and quasi-Newton [13], etc. The NS-MIA [14], GS, SOR [15], and quasi-Newton [16] based detectors have been also proposed for XL-MIMO systems. The series and iterative method-based approximate detectors [8]–[16] efficiently implement the ZF and MMSE detectors but have the same asymptotic run-time complexity [17]. The multi-user data detection in uplink massive MIMO networks can be formulated as a high-dimensional regression problem where users data/ design parameter, $\mathbf{x} \in \mathbb{C}^{U\times 1}$, is to be recovered from received signal/ observation, $\mathbf{y} \in \mathbb{C}^{M\times 1}$, using uplink channel/ regression matrix $\mathbf{Z} \in \mathbb{C}^{M\times U}$, $M \gg U$.

The sampling and sketching-based [18] techniques offer a faster and approximate solution to the high dimensional regression problem via dimensionality reduction. The input matrix $\mathbf{Z}$ and observation vector $\mathbf{y}$ are sub-sampled by choosing K rows, $K \ll M$ in sampling-based techniques, whereas $\mathbf{Z}$, $\mathbf{y}$ are projected onto a random matrix of size $K \times M$ in sketching-based techniques. Sampling-based approach is preferred over sketching [19], as they are faster, preserve the sparsity of input matrices, and do not require the knowledge of the complete observation to reduce the run-time complexity.

In the context of approximate signal detection in uplink massive MIMO systems, sampling techniques perform equalization using selected entries of the channel matrix and received signal. This has potential to help to recover the transmitted information at a faster run-time than ZF, MMSE, and approximate linear detectors [8]–[16], with nominal approximation loss. Hence, this work focuses on using the advantages of the sampling-based approach for data detection in uplink massive MIMO networks. The key contributions are

- A novel sampling-based fast detection framework using rescaled Kronecker volume sampling (RKVS).
- RKVS detector for uplink massive MIMO networks with faster asymptotic run-time complexity than ZF detector.

- Theoretical and numerical performance analysis of the proposed RKVS detector.

Next section introduces the notation, system model, and rescaled volume sampling.

II. System Description

The notations used in this work are described next, followed by system model and a summary of rescaled volume sampling.

A. Notation and Background

The notations used throughout this paper are as follows: Complex and real fields are denoted by $\mathbb{C}$ and $\mathbb{R}$, respectively. The expectation and probability operations are denoted as $\mathbb{E}[.]$ and $\Pr[.]$. Tensors, matrices, vectors, and scalars are denoted by calligraphic, boldface uppercase, boldface lowercase, and regular face alphabets respectively. For a matrix $\mathbf{A}$, the row i, column j and ijth entry is denoted using $\mathbf{A}_{(i,:)}$, $\mathbf{A}_{(:,j)}$ and A_{ij} respectively. The operators conjugate transpose, pseudo-inverse, and determinant on a matrix $\mathbf{A}$ is denoted using $\mathbf{A}^{\mathrm{H}}$, $\mathbf{A}^{\dagger}$ and $|\mathbf{A}|$, respectively. The column-wise vectorization operation on matrix $\mathbf{A} \in \mathbb{C}^{I\times J}$ is denoted by $\mathrm{vec}(\mathbf{A}) \in \mathbb{C}^{IJ\times 1}$. A set of indices $\{1, 2, \dots K\}$ is denoted as $\langle K\rangle$. The symbols '$\otimes$', '$\odot$' and '$:=$' denote Kronecker product, Khatri-Rao product [20] and 'defined as' respectively. A Bernoulli trial with success probability p is denoted using $\mathrm{Bernoulli}(p)$. The Definitions II.1 and II.2 stated next from linear algebra are used in the analysis.

Definition II.1 (Leverage score sampling (LSS) [21])**.** *Let $\mathbf{U} \in \mathbb{R}^{N\times D}$ denote a matrix with top D left singular vectors of $\mathbf{Z} \in \mathbb{R}^{N\times D}$ as columns, such that $l_i := \|\mathbf{U}_{(i,:)}\|_2^2$ denotes the ith leverage score of $\mathbf{Z}$. Then, leverage score sampling selects a subset of rows from $\mathbf{Z}$, via the probability distribution $(q_1, q_2, \dots q_I)$, where $q_i \geq l_i/D$, for $i \in \{1, 2, \dots I\}$ denotes the probability of sampling ith row from $\mathbf{Z}$.*

Definition II.2 (Volume Sampling (VS) [22])**.** *For a matrix $\mathbf{Z} \in \mathbb{C}^{N\times D}$, the volume sampling selects a small subset of rows from $\mathbf{Z}$ with probability proportional to volume of the submatrix (volume of a matrix $\mathbf{Z}$ refers to $|\mathbf{Z}^H\mathbf{Z}|$). The size K volume sampling on $\mathbf{Z}$ is denoted as VolumeSample$(\mathbf{Z}, K)$ and gives sampled row indices as output.*

B. System Model

Consider an uplink multi-user massive MIMO communication network where U single antenna users are simultaneously transmitting to a BS with M antennas where $M \gg U$. Each element of the information symbol vector $\mathbf{S}_{(:,u)} \in \mathbb{C}^{L\times 1}$ of user u, $1 \leq u \leq U$ is encoded using a coding vector $\mathbf{E}_{(:,u)} \in \mathbb{C}^{P\times 1}$. The uplink channel $\mathbf{H} \in \mathbb{C}^{M\times U}$ between U users and the BS is assumed to be flat fading, Rayleigh. The component of received signal $\mathcal{Y} \in \mathbb{C}^{M\times P\times L}$ at the BS corresponding to information symbol l, $1 \leq l \leq L$ and encoding symbol p, $1 \leq p \leq P$ is given as

$$\mathcal{Y}_{(:,l,p)} = \sum_{u=1}^{U} \mathbf{H}_{(:,u)} E_{pu} S_{ul} = \mathbf{H} D_l(\mathbf{S}) \mathbf{E}^{\mathrm{H}}_{(:,p)}, \qquad (1)$$

where $\mathbf{H}_{(:,u)} \in \mathbb{C}^{M\times 1}$ denotes uplink channel between user u and the BS, $D_l(\mathbf{S}) \in \mathbb{C}^{U\times U}$ denotes a diagonal matrix with elements of vector $\mathbf{S}_{(l,:)}$ as principal diagonal. The component $\mathbf{Y}_l = [\mathcal{Y}_{(:,l,1)}\ \mathcal{Y}_{(:,l,2)}\ \dots\ \mathcal{Y}_{(:,l,P)}] \in \mathbb{C}^{M\times P}$ of received signal corresponding to users encoded symbol l from (1) is

$$\mathbf{Y}_l = \mathbf{H} D_l(\mathbf{S}) \mathbf{E}^{\mathrm{H}}. \qquad (2)$$

Use the relation $\mathrm{vec}(\mathbf{A}\mathbf{M}\mathbf{B}^{\mathrm{H}}) = (\mathbf{B} \odot \mathbf{A})\mathbf{m}$ [20], where $\mathbf{M}$ is a diagonal matrix with diagonal entries $\mathbf{m}$ to vectorize $\mathbf{Y}_l$ in (2) as $\mathbf{y}_l = \mathrm{vec}(\mathbf{Y}_l)$. Let $[\mathcal{Y}]_L \in \mathbb{C}^{L\times MP}$ denote matricization of received signal tensor $\mathcal{Y} \in \mathbb{C}^{M\times P\times L}$ along mode L, obtained by stacking the fibers along the mode L as columns. Then $[\mathcal{Y}]_L^{\mathrm{H}} = [\mathbf{y}_1\ \mathbf{y}_2\ \dots\ \mathbf{y}_L] \in \mathbb{C}^{MP\times L}$ is given as

$$[\mathcal{Y}]_L^{\mathrm{H}} = (\mathbf{E} \odot \mathbf{H})\mathbf{S}^{\mathrm{H}}. \qquad (3)$$

Let $\mathbf{I} \in \mathbb{R}^{L\times L}$ denote identity matrix. Use the relation $\mathrm{vec}(\mathbf{A}\mathbf{D}\mathbf{B}^{\mathrm{H}}) = (\mathbf{B} \otimes \mathbf{A})\mathrm{vec}(\mathbf{D})$ [20] to vectorize $[\mathcal{Y}]_L^{\mathrm{H}}$ as

$$\mathbf{y} = \mathbf{I} \otimes (\mathbf{E} \odot \mathbf{H})\mathbf{s}, \qquad (4)$$

where $\mathbf{y} = \mathrm{vec}([\mathcal{Y}]_L^{\mathrm{H}}) \in \mathbb{C}^{MPL\times 1}$ and $\mathbf{s} = \mathrm{vec}(\mathbf{S}^{\mathrm{H}}) \in \mathbb{C}^{LU\times 1}$. The ZF detector statistic [7] $\mathbf{s}_{\mathrm{ZF}}$ for channel matrix $\mathbf{H}$, coding matrix $\mathbf{E}$ and received signal $\mathbf{y}$ is given as

$$\mathbf{s}_{\mathrm{ZF}} = \arg\min_{\mathbf{s}\in\mathbb{C}^{LU\times 1}} \|\mathbf{y} - \mathbf{I} \otimes (\mathbf{E} \odot \mathbf{H})\mathbf{s}\|_2. \qquad (5)$$

The solution to (5) is well known to be $\mathbf{s}_{\mathrm{ZF}} = (\mathbf{I} \otimes (\mathbf{E} \odot \mathbf{H}))^{\dagger}\mathbf{y}$ with a run-time complexity of $O(MPL^3U^2)$, i.e., SVD complexity of $\mathbf{I} \otimes (\mathbf{E} \odot \mathbf{H}) \in \mathbb{C}^{MPL\times LU}$. This is significantly high for large values of M and P. The next subsection briefly reviews a sampling-based approximation method with faster asymptotic run-time for high dimensional regression problems.

C. Approximate Regression via Rescaled Volume Sampling

The rescaled volume sampling [23] approximates the regression problem $\arg\min_{\mathbf{x}} \|\mathbf{Z}\mathbf{x} - \mathbf{y}\|_2$ where $\mathbf{Z} \in \mathbb{C}^{N\times D}$, $\mathbf{y} \in \mathbb{C}^{N\times 1}$ and $N \gg D$ in two steps. Sample and rescale a subset of rows from $\mathbf{Z}$, $\mathbf{y}$ to construct $\mathbf{Z}_K$, $\mathbf{y}_K$ followed by solving $\arg\min_{\mathbf{x}} \|\mathbf{Z}_K\mathbf{x} - \mathbf{y}_K\|_2$. Let $r = \{r_1, r_2, \dots r_N\}$ denote a discrete probability distribution over the index set $\langle N\rangle$. The sampling and rescaling of rows from $\mathbf{Z}$ and $\mathbf{y}$ is performed using matrix $\mathbf{T}_{\boldsymbol{\eta}}^{1/2} \in \mathbb{R}^{N\times N}$. It is constructed using an index set $\boldsymbol{\eta} = \{\eta_1, \eta_2, \dots \eta_K\}$ of size K, sampled with replacement from $\langle N\rangle$ as follows.

$$\mathbf{T}_{\boldsymbol{\eta}}^{1/2} = \sum_{k=1}^{K} \frac{\mathbf{e}_{\eta_k}\mathbf{e}_{\eta_k}^{\mathrm{H}}}{\sqrt{r_{\eta_k}}}, \text{ w.p.} \frac{|\mathbf{Z}^{\mathrm{H}}\mathbf{T}_{\boldsymbol{\eta}}\mathbf{Z}| \prod_{k=1}^{K} r_{\eta_k}}{A} \qquad (6)$$

where $\mathbf{e}_i \in \mathbb{R}^{N\times 1}$ denotes ith standard ordered basis vector of $\mathbb{R}^{N\times 1}$ and 'w.p.' stands for 'with probability'. The sampling matrix is obtained using the Determinantal rejection sampling algorithm [23]. Let $\langle N\rangle^K$ denote all the possible size K index set sampled with replacement from $\langle N\rangle$. The normalization constant A for the rescaled volume sampling distribution is obtained by summing the sampling probabilities of all the possible size K index sets $\boldsymbol{\eta}$ as follows [23, Proposition 2]

$$A = \sum_{\boldsymbol{\eta}\in\langle N\rangle^K} |\mathbf{Z}^{\mathrm{H}}\mathbf{T}_{\boldsymbol{\eta}}\mathbf{Z}| \prod_{k=1}^{K} r_{\eta_k} = (D)! \binom{K}{D} |\mathbf{Z}^{\mathrm{H}}\mathbf{Z}|. \qquad (7)$$

Further, the subsampled design matrix/ observation vector $\mathbf{Z}_K := \mathbf{T}_{\boldsymbol{\eta}}^{1/2}\mathbf{Z}$, $\mathbf{y}_K := \mathbf{T}_{\boldsymbol{\eta}}^{1/2}\mathbf{y}$ are used to formulate the rescaled volume sampling-based approximate problem as $\mathbf{x}_{\text{RVS}} = \arg\min_{\mathbf{x}\in\mathbb{C}^{D\times 1}}\|\mathbf{Z}_K\mathbf{x} - \mathbf{y}_K\|_2$. The solution $\mathbf{x}_{\text{RVS}} = \mathbf{Z}_K^{\dagger}\mathbf{y}_K$ is obtained at an overall (including sampling overhead) run-time complexity of $O(ND^2 + (4D^2 + K)D^2)$ [23, Theorem 6]. Further, the obtained weight vector $\mathbf{x}_{\text{RVS}}$ is an unbiased estimator of optimal weight vector $\mathbf{x}^*$, i.e., the solution to $\arg\min_{\mathbf{x}}\|\mathbf{Z}\mathbf{x} - \mathbf{y}\|_2$ [23, Theorem 3].

III. Rescaled Kronecker Volume Sampling (RKVS) Detector

This section presents a faster multi-user data detector for uplink massive MIMO networks based on a scalable extension of rescaled volume sampling. Proposed RKVS detector is discussed next, followed by its quality of approximation/ computational complexity in sections III-B/ III-C.

A. Approximate multi-user data detector

The detection problem in (5) is modified to exploit the Kronecker product structure. Let $\mathbf{C} \in \mathbb{R}^{U^2\times U}$ be a column selection matrix such that $\mathbf{E}\odot\mathbf{H} = (\mathbf{E}\otimes\mathbf{H})\mathbf{C}$. The matrix $\mathbf{I}\otimes(\mathbf{E}\odot\mathbf{H})$ in (5) is rearranged to

$$\mathbf{I}\otimes(\mathbf{E}\odot\mathbf{H}){=}\mathbf{I}\otimes((\mathbf{E}\otimes\mathbf{H})\mathbf{C}){=}(\mathbf{I}\otimes\mathbf{E}\otimes\mathbf{H})(\mathbf{I}\otimes\mathbf{C}), \quad (8)$$

using properties $(\mathbf{A}\otimes\mathbf{C})(\mathbf{B}\otimes\mathbf{D}) = \mathbf{AB}\otimes\mathbf{CD}$ and $(\mathbf{A}\otimes\mathbf{C})(\mathbf{B}\odot\mathbf{D}) = \mathbf{AB}\odot\mathbf{CD}$ from [20]. Let $\mathbf{x} := (\mathbf{I}\otimes\mathbf{C})\mathbf{s}$. Equivalent detection problem using (8) and $\mathbf{x}$ is

$$\mathbf{x}_{\text{ZF}} = \arg\min_{\mathbf{x}\in\mathbb{C}^{LU^2}}\|\mathbf{y} - \mathbf{Z}\mathbf{x}\|_2, \quad (9)$$

where $\mathbf{Z} = \mathbf{I}\otimes\mathbf{E}\otimes\mathbf{H}$, $\mathbf{Z}\in\mathbb{C}^{N\times D}$, $N = MPL$ and $D = LU^2$. The obtained solution $\mathbf{x}_{\text{ZF}}$ is used to get the detector $\mathbf{s}_{\text{ZF}}$ as $\mathbf{s}_{\text{ZF}} = (\mathbf{I}\otimes\mathbf{C})^{-1}\mathbf{x}_{\text{ZF}} = (\mathbf{I}\otimes\mathbf{C})^{\mathrm{H}}\mathbf{x}_{\text{ZF}}$. The rescaled volume sampling approach discussed in section II-C is employed to compute an approximate solution to the problem in (9). A key idea to propose a scalable approach that obtain an equivalent sampling distribution for $\mathbf{Z}$ using factor matrices $\mathbf{I}$, $\mathbf{E}$ and $\mathbf{H}$. This is achieved by exploiting the Kronceker product structure of $\mathbf{Z}$. The selection probability r for the row indices of $\mathbf{Z}$ without explicitly constructing $\mathbf{Z}$ is obtained in proposition 1.

Proposition 1. *Let a discrete probability distribution over the row indices of* $\mathbf{I}$, $\mathbf{E}$ *and* $\mathbf{H}$ *be denoted by* $r^{(\mathbf{I})} := \{r_1^{(\mathbf{I})}, r_2^{(\mathbf{I})}, \dots, r_L^{(\mathbf{I})}\}$, $r^{(\mathbf{E})} := \{r_1^{(\mathbf{E})}, r_2^{(\mathbf{E})}, \dots, r_P^{(\mathbf{E})}\}$ *and* $r^{(\mathbf{H})} := \{r_1^{(\mathbf{H})}, r_2^{(\mathbf{H})}, \dots, r_M^{(\mathbf{H})}\}$ *respectively where* $r_j^{(\mathbf{I})}$ *indicates the probability of sampling row* j *from matrix* $\mathbf{I}$. *Then,* $r^{(\mathbf{Z})} := r^{(\mathbf{I})}\otimes r^{(\mathbf{E})}\otimes r^{(\mathbf{H})}$ *is a discrete distribution over the row indices of* $\mathbf{Z} = \mathbf{I}\otimes\mathbf{E}\otimes\mathbf{H}$.

Proposition 1 gives a size K sampled index set $\boldsymbol{\eta}$ for rows of $\mathbf{Z}$, according to distribution in (6). Sample the row index sets $\boldsymbol{\eta}^{(\mathbf{I})} = \{\eta_k^{(\mathbf{I})}\}$, $\boldsymbol{\eta}^{(\mathbf{E})} = \{\eta_k^{(\mathbf{E})}\}$ and $\boldsymbol{\eta}^{(\mathbf{H})} = \{\eta_k^{(\mathbf{H})}\}$, $1\le k\le K$ with replacement from the row indices of $\mathbf{I}$, $\mathbf{E}$ and $\mathbf{H}$ respectively. The sampling is done with replacement, according to corresponding distributions $r^{(\mathbf{I})}$, $r^{(\mathbf{E})}$ and $r^{(\mathbf{H})}$. Further, the sampled index set for the rows of matrix $\mathbf{Z}$, i.e., $\boldsymbol{\eta}^{(\mathbf{Z})} = \{\eta_k^{(\mathbf{Z})}\}$ is constructed using $\boldsymbol{\eta}^{(\mathbf{I})}$, $\boldsymbol{\eta}^{(\mathbf{E})}$ and $\boldsymbol{\eta}^{(\mathbf{H})}$ as

$$\eta_k^{(\mathbf{Z})} = \eta_k^{(\mathbf{H})} + (\eta_k^{(\mathbf{E})})M + (\eta_k^{(\mathbf{I})})MP. \quad (10)$$

The marginal probability of $\eta_k^{(\mathbf{Z})}\in\boldsymbol{\eta}^{(\mathbf{Z})}$ is given as product of marginals $\Pr[\eta_k^{(\mathbf{I})}\in\boldsymbol{\eta}^{(\mathbf{I})}]$, $\Pr[\eta_k^{(\mathbf{E})}\in\boldsymbol{\eta}^{(\mathbf{E})}]$ and $\Pr[\eta_k^{(\mathbf{H})}\in\boldsymbol{\eta}^{(\mathbf{H})}]$. The sets $r^{(\mathbf{Z})}$ and $\boldsymbol{\eta}^{(\mathbf{Z})}$ are denoted by r and $\boldsymbol{\eta}$ in rest of the paper for brevity. Thus, the sampling matrix $\mathbf{T}_{\boldsymbol{\eta}}^{1/2}$ for the rows of $\mathbf{Z}$ is expressed in terms of sampling matrices $\mathbf{T}_{\boldsymbol{\eta}^{(\mathbf{I})}}^{1/2}$, $\mathbf{T}_{\boldsymbol{\eta}^{(\mathbf{E})}}^{1/2}$ and $\mathbf{T}_{\boldsymbol{\eta}^{(\mathbf{H})}}^{1/2}$ of $\mathbf{I}$, $\mathbf{E}$ and $\mathbf{H}$ respectively using (10) as

$$\mathbf{T}_{\boldsymbol{\eta}}^{1/2} = \left((\mathbf{T}_{\boldsymbol{\eta}^{(\mathbf{I})}}^{1/2})^{\mathrm{H}}\odot(\mathbf{T}_{\boldsymbol{\eta}^{(\mathbf{E})}}^{1/2})^{\mathrm{H}}\odot(\mathbf{T}_{\boldsymbol{\eta}^{(\mathbf{H})}}^{1/2})^{\mathrm{H}}\right)^{\mathrm{H}}. \quad (11)$$

Next, the obtained sampled index set $\boldsymbol{\eta}$ is accepted with probability proportional to $\frac{|\mathbf{Z}^{\mathrm{H}}\mathbf{T}_{\boldsymbol{\eta}}\mathbf{Z}|}{A}$. The RKVS based multi-user data detector for (9) is summarized in Algorithm 1. The sampling distributions $r^{(\mathbf{I})}$, $r^{(\mathbf{E})}$ and $r^{(\mathbf{H})}$ on the row indices of $\mathbf{I}$, $\mathbf{E}$ and $\mathbf{H}$ is chosen as follows: $r^{(\mathbf{I})} = \frac{1}{L}\{1, 1, \dots 1\}$, $r^{(\mathbf{E})} = \frac{1}{P}\{l_1^{(\mathbf{E})}, l_2^{(\mathbf{E})}, \dots l_P^{(\mathbf{E})}\}$, and $r^{(\mathbf{H})} = \frac{1}{M}\{l_1^{(\mathbf{H})}, l_2^{(\mathbf{H})}, \dots l_M^{(\mathbf{H})}\}$. Here $\{l_j^{(\mathbf{A})}\}$ denote the leverage score (refer definition II.1) corresponding to the row j of a given matrix $\mathbf{A}$. The choice is motivated by a design criteria $\mathbb{E}[\mathbf{Z}_K^{\mathrm{H}}\mathbf{Z}_K] = \mathbf{Z}^{\mathrm{H}}\mathbf{Z}$ [23].

B. Scalability and Quality of Approximation

Lemma III.1 claims that Algorithm 1 samples the rows from $\mathbf{Z}$ according to (6), without complete knowledge of $\mathbf{Z}$.

Lemma III.1. *Let* $\mathbf{Z}\in\mathbb{C}^{N\times D}$ *be a Kronecker design matrix where* $\mathbf{Z} = \mathbf{I}\otimes\mathbf{E}\otimes\mathbf{H}$. *Then, the size* K *index set* $\boldsymbol{\eta}$ *obtained by sampling with replacement from row indices of* $\mathbf{Z}$ *using Algorithm 1 has the same joint sampling distribution as the one obtained from size* K *rescaled volume sampling using [23, Determinantal Rejection sampling].*

Proof. The proof follows by a key observation that Algorithm 1 and the Determinantal Rejection sampling [23] follow a similar approach to obtain a size K sampled index set from the row indices of $\mathbf{Z}$. Firstly, a size $B = \max\{4D^2, K\}$ sampled index set is obtained using rescaled volume sampling [23, eq. (5)], resulting into corresponding subsampled design matrix $\mathbf{Z}_B$. This is followed by size K volume sampling on $\mathbf{Z}_B$ (refer definition II.2) to yield size K sampled index set $\boldsymbol{\eta}$. The results from [23, Lemma 7] show that the two step sampling procedure is equivalent to a direct size K rescaled volume sampling on $\mathbf{Z}$. Hence it suffices to prove that the acceptance probability of sampled index set at the end of first stage, line 8 in Algorithm 1, is the same for both the algorithms. The row i of $\mathbf{Z}_B$ in Algorithm 1 (line 7) is given as $(\mathbf{Z}_B)_{(i,:)} = (\mathbf{I}_B)_{(i,:)}\otimes(\mathbf{E}_B)_{(i,:)}\otimes(\mathbf{H}_B)_{(i,:)}$ for $i = 1\dots B$, where $\mathbf{I}_B = \mathbf{T}_{\boldsymbol{\eta}^{(\mathbf{I})}}^{1/2}\mathbf{I}$, $\mathbf{E}_B = \mathbf{T}_{\boldsymbol{\eta}^{(\mathbf{E})}}^{1/2}\mathbf{E}$ and $\mathbf{H}_B = \mathbf{T}_{\boldsymbol{\eta}^{(\mathbf{H})}}^{1/2}\mathbf{H}$. Further, $\mathbf{Z}_B$ is written in terms of $\mathbf{I}$, $\mathbf{E}$ and $\mathbf{H}$ as

$$\begin{aligned}\mathbf{Z}_B &= \left((\mathbf{T}_{\boldsymbol{\eta}^{(\mathbf{I})}}^{1/2}\mathbf{I})^{\mathrm{H}}\odot(\mathbf{T}_{\boldsymbol{\eta}^{(\mathbf{E})}}^{1/2}\mathbf{E})^{\mathrm{H}}\odot(\mathbf{T}_{\boldsymbol{\eta}^{(\mathbf{H})}}^{1/2}\mathbf{H})^{\mathrm{H}}\right)^{\mathrm{H}} \quad (12)\\ &= \left((\mathbf{I}\otimes\mathbf{E}\otimes\mathbf{H})^{\mathrm{H}}\left((\mathbf{T}_{\boldsymbol{\eta}^{(\mathbf{I})}}^{1/2})^{\mathrm{H}}\odot(\mathbf{T}_{\boldsymbol{\eta}^{(\mathbf{E})}}^{1/2})^{\mathrm{H}}\odot(\mathbf{T}_{\boldsymbol{\eta}^{(\mathbf{H})}}^{1/2})^{\mathrm{H}}\right)\right)^{\mathrm{H}}\\ &= \mathbf{T}_{\boldsymbol{\eta}}^{1/2}\mathbf{Z}. \quad (13)\end{aligned}$$

Here (12), (13) follows from properties of Khatri-Rao product [20] and definition of $\mathbf{Z}$ in (9) and $\mathbf{T}_{\boldsymbol{\eta}}^{1/2}$ in (11). The denominator term Q in line 7 of Algorithm 1 is resolved as

$$Q = |\mathbf{E}^{\mathrm{H}}\mathbf{E}|^{LU} |\mathbf{H}^{\mathrm{H}}\mathbf{H}|^{LU} = |(\mathbf{I} \otimes \mathbf{E} \otimes \mathbf{H})^{\mathrm{H}} (\mathbf{I} \otimes \mathbf{E} \otimes \mathbf{H})|,$$

by using the relation $|\mathbf{A} \otimes \mathbf{B}| = |\mathbf{A}|^J |\mathbf{B}|^I$ for $\mathbf{A} \in \mathbb{C}^{I \times I}$ and $\mathbf{B} \in \mathbb{C}^{J \times J}$ [20]. Finally, the fact that acceptance probability at the end of first stage sampling in [23, Determinantal Rejection sampling] is given by $\frac{|(1/B)\mathbf{Z}^{\mathrm{H}}\mathbf{T}_{\boldsymbol{\eta}}\mathbf{Z}|}{|\mathbf{Z}^{\mathrm{H}}\mathbf{Z}|}$ completes the proof. $\square$

The next theorem shows that the proposed RKVS detector $\mathbf{s}_{\text{RKVS}}$ is an unbiased estimator of the ZF detector statistic $\mathbf{s}_{\text{ZF}}$.

Theorem III.2 (Unbiasedness)**.** *The proposed RKVS detector $\mathbf{s}_{\mathit{RKVS}}$ in Algorithm 1 is an unbiased estimator of the ZF detector statistic $\mathbf{s}_{\mathit{ZF}}$, i.e., $\mathbb{E}[\mathbf{s}_{\mathit{RKVS}}] = \mathbf{s}_{\mathit{ZF}}$, for a given channel matrix $\mathbf{H}$, code matrix $\mathbf{E}$ in the uplink massive MIMO communication networks* (4)*.*

Proof. From Lemma III.1, the proposed detector $\mathbf{s}_{\text{RKVS}}$ is equivalent to the one obtained using rescaled volume sampling (section II-C). Rest of the proof follows [23, Theorem 3]. $\square$

Algorithm 1: RKVS based multi-user data detector

Data: Channel matrix $\mathbf{H} \in \mathbb{C}^{M \times U}$, Code matrix $\mathbf{E} \in \mathbb{C}^{P \times U}$, received signal $\mathbf{y}$, sample size K

Result: Multi-user detector $\mathbf{s}_{\text{RKVS}}$

1 $B \leftarrow \max\{4L^2U^4, K\}$;

2 $Q \leftarrow |\mathbf{E}^{\mathrm{H}}\mathbf{E}|^{LU} |\mathbf{H}^{\mathrm{H}}\mathbf{H}|^{LU}$;

3 Compute Leverage scores of $\mathbf{H}$ and $\mathbf{E}$ and assign to $r^{(\mathbf{H})}$ and $r^{(\mathbf{E})}$; `// see Defn. II.1`

4 $r = r^{(\mathbf{I})} \otimes r^{(\mathbf{E})} \otimes r^{(\mathbf{H})}$, for $r^{(\mathbf{I})} = \frac{1}{L}\{1, 1, \dots 1\}$;

5 **repeat**

6   Sample size B index sets $\boldsymbol{\eta}^{(\mathbf{E})}$, $\boldsymbol{\eta}^{(\mathbf{H})}$ and $\boldsymbol{\eta}^{(\mathbf{I})}$ i.i.d with replacement from $\langle P \rangle$, $\langle M \rangle$ and $\langle L \rangle$ using distributions $r^{(\mathbf{E})}$, $r^{(\mathbf{H})}$ and $r^{(\mathbf{I})}$ respectively;

7   Construct $\mathbf{E}_B := \mathbf{T}_{\boldsymbol{\eta}^{(\mathbf{E})}}^{1/2}\mathbf{E}$, $\mathbf{H}_B := \mathbf{T}_{\boldsymbol{\eta}^{(\mathbf{H})}}^{1/2}\mathbf{H}$, $\mathbf{I}_B := \mathbf{T}_{\boldsymbol{\eta}^{(\mathbf{I})}}^{1/2}\mathbf{I}$ and $\mathbf{Z}_B$ using $(\mathbf{Z}_B)_{(i,:)} = (\mathbf{I}_B)_{(i,:)} \otimes (\mathbf{E}_B)_{(i,:)} \otimes (\mathbf{H}_B)_{(i,:)}$ for $i = 1 \dots B$ and sample $\mathit{Accept} \sim$ Bernoulli $\left(\frac{|(1/B)\mathbf{Z}_B^{\mathrm{H}}\mathbf{Z}_B|}{Q}\right)$

8 **until** $\mathit{Accept} = \mathit{True}$;

9 **if** $B > K$ **then**

10     $\boldsymbol{\eta} \leftarrow$ VolumeSample$(\mathbf{Z}_B, K)$; `// see Defn. II.2`

11   Construct $\mathbf{T}_{\boldsymbol{\eta}}^{1/2}$ from $\boldsymbol{\eta}$ and r using (6);

12   Obtain $\mathbf{Z}_K$ by sampling the rows corresponding to $\boldsymbol{\eta}$ from $\mathbf{Z}_B$, $\mathbf{y}_K \leftarrow \mathbf{T}_{\boldsymbol{\eta}}^{1/2}\mathbf{y}$;

13 **else**

14   Construct $\mathbf{T}_{\boldsymbol{\eta}}^{1/2}$ (11) from $\mathbf{T}_{\boldsymbol{\eta}^{(\mathbf{E})}}^{1/2}$, $\mathbf{T}_{\boldsymbol{\eta}^{(\mathbf{H})}}^{1/2}$ and $\mathbf{T}_{\boldsymbol{\eta}^{(\mathbf{I})}}^{1/2}$;

15     $\mathbf{Z}_K \leftarrow \mathbf{Z}_B$, $\mathbf{y}_K \leftarrow \mathbf{T}_{\boldsymbol{\eta}}^{1/2}\mathbf{y}$;

16 **end**

17 $\mathbf{x}_{\text{RKVS}} \leftarrow (\mathbf{Z}_K)^{\dagger}\mathbf{y}_K$, $\mathbf{s}_{\text{RKVS}} \leftarrow (\mathbf{I} \otimes \mathbf{C}^{\mathrm{H}})\mathbf{x}_{\text{RKVS}}$;

18 **return** $\mathbf{s}_{\text{RKVS}}$

C. Computational Complexity Analysis

The Algorithm 1 consists of components with deterministic run-time, like the pre-processing in lines 1-4, volume sampling in line 10-12, regression in line 17, and probabilistic run-time in lines 5-8. The next theorem gives the asymptotic time complexity of Algorithm 1 by bounding the number of iterations of lines 5-8 known as the rejection sampling loop.

Theorem III.3. *The asymptotic run-time complexity of the RKVS detector in Algorithm 1 operating at sample size K for a given channel matrix $\mathbf{H} \in \mathbb{C}^{M \times U}$ and code matrix $\mathbf{E} \in \mathbb{C}^{P \times U}$ in an uplink massive MIMO communication network* (4) *is $O((4L^2U^4 + 2K)L^2U^4 + (M+P)U^2)\log(1/\delta))$ with probability at least $1 - \delta$.*

Proof. Let w denote the number of iterations of the rejection sampling loop. To bound the value of w, the expected value of acceptance probability is resolved as

$$\sum_{\boldsymbol{\eta} \in \langle N \rangle^B} \prod_{b=1}^{B} r_{\eta_b} \frac{|(1/B)\mathbf{Z}^{\mathrm{H}}\mathbf{T}_{\boldsymbol{\eta}}\mathbf{Z}|}{|\mathbf{Z}^{\mathrm{H}}\mathbf{Z}|} \stackrel{(a)}{=} \frac{B(B-1)\dots(B-D+1)}{B^D} \geq (B - D^2)/B, \tag{14}$$

where (a) results from substituting the normalization constant (7). Equation (14) is lower bounded by $\frac{3}{4}$ as $B = \max\{4D^2, K\}$. Further application of Markov inequality leads to $w \leq \log(\frac{1}{\delta})/\log(\frac{4}{3})$ with probability at least $1 - \delta$ [23]. The operations inside the rejection sampling loop and the corresponding run-time complexities are given as follows

1) Construction of $\mathbf{Z}_B$ involves obtaining the value of B rows, with D elements per row. Hence it has the complexity $O(BD)$.
2) Calculating the acceptance probability involves computing $|\mathbf{Z}_B^{\mathrm{H}}\mathbf{Z}_B|$ which has complexity $O(BD^2)$.

Further, the step 10 of Algorithm 1 performs standard K sized volume sampling on $\mathbf{Z}_B \in \mathbb{C}^{B \times D}$ and has a complexity of $O(BD^2)$ [22]. Hence the overall complexity of the rejection sampling loop and standard volume sampling part (lines 5-16) of the Algorithm 1 is $O(BD^2\log(1/\delta))$ which is further resolved using $B \leq (4D^2 + K)$ as $O((4D^2+K)D^2\log(1/\delta))$. Computing Q, and distributions $r^{(\mathbf{H})}$, $r^{(\mathbf{E})}$ for given matrices $\mathbf{H}$ and $\mathbf{E}$ respectively is of complexity $O((M+P)U^2)$. Substituting $D = LU^2$ gives the overall complexity of Algorithm 1 as $O((M+P)U^2 + (4L^2U^4 + K)L^2U^4 + KL^2U^4)$ or equivalently $O((4L^2U^4+2K)L^2U^4+(M+P)U^2)$ with high probability. The proposed RKVS detector has lower asymptotic run-time complexity than ZF detector in uplink massive MIMO systems for large M, number of BS antenna. $\square$

The complexities of the RKVS and baseline detectors is summarized in Table I and is further discussed in next section.

IV. Performance Analysis and Discussion

This section presents baseline detectors, compares the run-time complexity, error performance of the RKVS detector with the ZF detector and its sampling-based approximations.

TABLE I: Asymptotic run-time of multi-user data detectors.

Detector	Time Complexity
$\mathbf{x}_{\text{ZF}}$ (9)	$O(MPL^3U^2)$
$\mathbf{x}_{\text{LSS}}$ (15)	$O\left((M+P)U^2 + L^3U^6 + KL^2U^4 + \text{poly}(MPL)\right)$
$\mathbf{x}_{\text{VS}}$ (16)	$O(MPL^3U^4 + KL^2U^4)$
$\mathbf{x}_{\text{RKVS}}$	$O((4L^2U^4 + 2K)L^2U^4 + (M+P)U^2)$

A. Baseline detectors and comparison with the RKVS detector

1) ZF detector [5]: Recall that the ZF multi-user data detector for equivalent problem in (9) is obtained to be $\mathbf{s}_{\text{ZF}} = (\mathbf{I} \otimes \mathbf{C})^{\text{H}}\mathbf{x}_{\text{ZF}}$ where $\mathbf{x}_{\text{ZF}}$ is given as

$$\mathbf{x}_{\text{ZF}} = \arg\min_{\mathbf{x}\in\mathbb{C}^{LU^2}} \|\mathbf{y} - (\mathbf{I}\otimes\mathbf{E}\otimes\mathbf{H})\mathbf{x}\|_2.$$

2) Leverage Score Sampling (LSS) detector: The work in [24] gives an efficient way to construct the sampling matrix on $\mathbf{Z} = \mathbf{I}\otimes\mathbf{E}\otimes\mathbf{H}$ by using the leverage scores of $\mathbf{I}$, $\mathbf{E}$ and $\mathbf{H}$. Let $\mathbf{T}_{\text{LSS}}$ denote the sampling matrix constructed on $\mathbf{Z}$ [24, Lemma 4.1]. Then, LSS detector for (9) is given as

$$\mathbf{x}_{\text{LSS}} = \arg\min_{\mathbf{x}\in\mathbb{C}^{LU^2}} \|\mathbf{T}_{\text{LSS}}\mathbf{y} - \mathbf{T}_{\text{LSS}}\mathbf{Z}\mathbf{x}\|_2. \quad (15)$$

3) Volume Sampling (VS) detector: The volume sampling method in [22] is employed to approximately solve the multi-user uplink data detection problem in (9) as follows. Let $\mathbf{T}_{\text{VS}}$ denote the sampling matrix constructed on $\mathbf{Z}$ using the algorithm [22, FastRegVol]. Then, VS detector for (9) is

$$\mathbf{x}_{\text{VS}} = \arg\min_{\mathbf{x}\in\mathbb{C}^{LU^2}} \|\mathbf{T}_{\text{VS}}\mathbf{y} - \mathbf{T}_{\text{VS}}\mathbf{Z}\mathbf{x}\|_2. \quad (16)$$

The detector $\mathbf{s}_{\mathbf{T}} \in \{\mathbf{s}_{\text{LSS}}, \mathbf{s}_{\text{VS}}\}$ is further obtained using $\mathbf{x}_{\mathbf{T}} \in \{\mathbf{x}_{\text{LSS}}, \mathbf{x}_{\text{VS}}\}$ as $\mathbf{s}_{\mathbf{T}} = (\mathbf{I}\otimes\mathbf{C})^{\text{H}}\mathbf{x}_{\mathbf{T}}$.

Asymptotic Run-Time Complexity Comparison: Table I compares the asymptotic run-time of the proposed RKVS detector with the detectors employing state-of-the-art leverage score [24] and volume sampling [22] based approximate regression. The RKVS detector in Algorithm 1 has a faster asymptotic run-time than the ZF and VS detector in multi-user uplink massive MIMO networks when $(4L^2U^4 + 2K)U^2 = o(MPL)$, where $o(.)$ stands for the *small-oh* notation [25], defined as $f(n) = o(g(n)) \implies f(n)/g(n) = 0$ as $n \to \infty$. Further, the added advantage of unbiasedness for RKVS detector compensates for the higher run-time complexity compared to the biased LSS detector [23].

B. Numerical Results for Error Performance

An uplink massive MIMO communication system with $U \in \{6, 12\}$ users simultaneously transmitting their data to an $M \in \{128, 256, 1024\}$ antenna BS is considered. Data of a user u has a symbol length $L = 8$, modulated using MPSK, BPSK in Fig. 1, 2a and 2c, and encoded using a coding vector $\mathbf{E}_{(:,u)} \in \mathbb{C}^{P\times 1}$ of length $P = 60$. The matrix $\mathbf{E}$ with coding vectors for users is generated as $E_{ij} = e^{-j2\pi\alpha}/\sqrt{P}$, where α is drawn from uniform distribution over interval $[0, 1]$. The uplink channel between users and the BS is assumed to be block fading, Rayleigh with log-normal shadowing of 10dB. The average bit error rate (BER) *v/s* SNR relation is used to compare the proposed and baseline detectors.

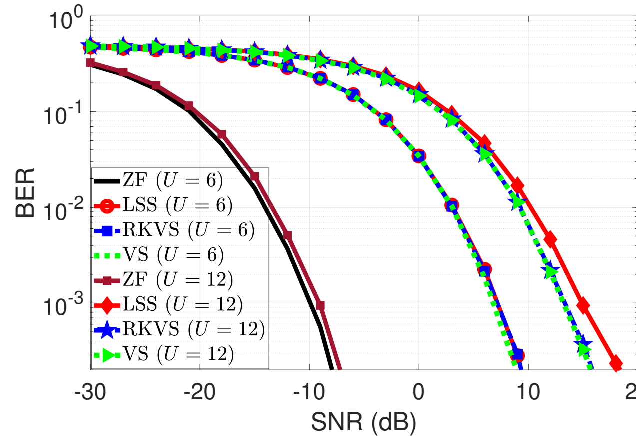

Fig. 1: BER *v/s* SNR performance comparison of proposed RKVS and baseline LSS, VS detectors for sample size $K = 1500$, BPSK modulation, $M = 128$ BS antennas, and users $U \in \{6, 12\}$ in an uplink massive MIMO network.

Fig. 1 compares the BER of proposed RKVS and baseline sampling based detectors with 128 BS antennas, at a sample size $K = 1500$, and serving $U = \{6, 12\}$ users. For a higher number of users RKVS detector performs better than the LSS detector and similar to the VS detector, which has a higher run-time complexity. This demonstrates the robust performance of the RKVS detector when the number of users in a network increases. Further, the BER rate of all the sampling based detectors increases with the number of users due to limited diversity gain per user in dense networks.

Fig. 2a compares the BER of RKVS and baseline sampling based detectors with 128 BS antennas, at sample sizes $K \in \{1500, 3000\}$, and serving 12 users. The RKVS detector has a BER better than the LSS and similar to the VS detector at $K = 1500$ highlighting the superior performance of RKVS detector compared to baseline sampling based detectors at low sample sizes. The BER of all sampling based detectors improves with an increase in the value of K from 1500 to 3000. The sample size K demonstrates the run-time *v/s* accuracy trade-off in RKVS detector (see Table I), a small K allows fast detection relevant in low-latency applications like autonomous driving, augmented reality, etc., a large value of K results in higher reliability useful for applications like critical and emergency services communications. Fig. 2b compares the performance of RKVS, at a sample size $K = 0.7 \times (MPL)$, and the ZF detector across the BPSK, 8PSK, and 32PSK modulation schemes in an uplink massive MIMO network with 12 users and 128 BS antennas. The BER of the RKVS detector follows a similar trend as the ZF detector with an increase in the modulation order from 2 (BPSK) to 32 (32PSK) demonstrating a comparable performance of RKVS and ZF detectors at different modulation schemes. Fig. 2c shows the effect of increasing the number of BS antennas M to extremely large values on the BER of the RKVS and the ZF detector. The BER of the RKVS detector is observed to be close to the ZF detector as M increases from 256 to 1024. This demonstrates the utility of the proposed RKVS detector in XL-MIMO systems with thousands of BS antennas. The

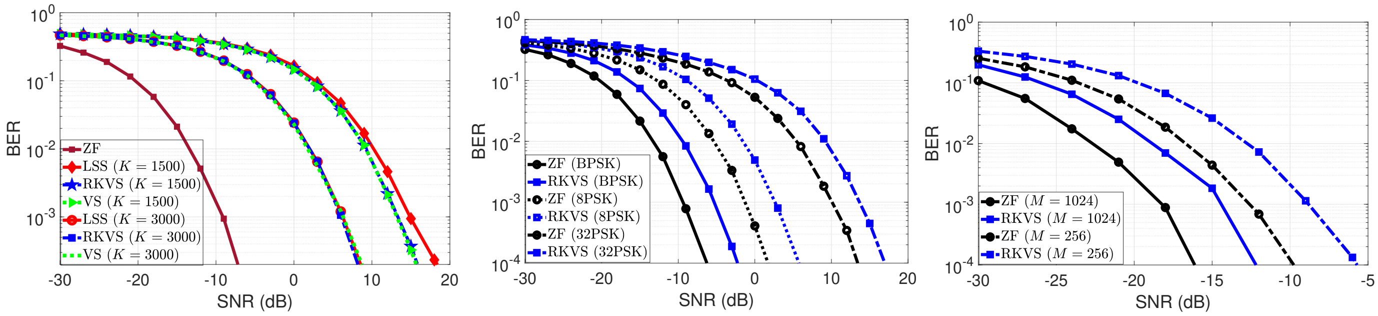

(a) (b) (c)

Fig. 2: BER *v/s* SNR performance comparison of the proposed RKVS detector in Algorithm 1 with baseline detectors, ZF (9), LSS (15), and VS (16) with U users, M BS antennas, sample size K in an uplink massive MIMO communication network, (2a) $U = 12$, $M = 128$, $K \in \{1500, 3000\}$ for BPSK modulation; (2b) $U = 12$, $M = 128$, $K = 0.7 \times (MPL)$ for BPSK, 8PSK, 32PSK modulation; (2c) $U = 12$, $M \in \{256, 1024\}$, $K = 0.7 \times (MPL)$ for BPSK modulation.

considered channel model for simulation corresponds to a non-LoS propagation environment [16]. The improved performance of both RKVS and ZF detectors with an increase in the number of BS antennas is attributed to a higher diversity order.

V. Conclusion

This work proposed a novel RKVS detector for multi-user uplink massive MIMO communication networks. Theoretical analysis proves that RKVS detector has a faster asymptotic run-time than the ZF detector. Moreover, the RKVS detector is an unbiased estimator of the optimal ZF detector statistic. Numerical results demonstrate BER performance of RKVS detector in close agreement to the ZF detector, with a performance trade-off and time complexity gain. The superior performance of the RKVS detector among the state-of-the-art sampling-based detectors at lower sample sizes is also observed. The same framework can be extended considering imperfect CSI to obtain a closed-form expression of BER, which can be further tailored to XL-MIMO systems.

References

[1] "CISCO Annual Internet Report 2018-2023. Accessed: March, 2020." [Online]. Available: www.cisco.com/c/en/us/solutions/collateral/executive-perspectives/annual-internet-report/white-paper-c11-741490.html.
[2] "Ericsson Mobility Report. Accessed: June, 2024." [Online]. Available: www.ericsson.com/en/reports-and-papers/mobility-report/reports.
[3] D. Astely, P. Von Butovitsch, S. Faxér, and E. Larsson, "Meeting 5G network requirements with massive MIMO," *Ericsson Technol. Rev.*, vol. 2022, no. 1, pp. 2–11, 2022.
[4] Z. Wang, J. Zhang, H. Du, W. E. I. Sha, B. Ai, D. Niyato, and M. Debbah, "Extremely large-scale MIMO: Fundamentals, challenges, solutions, and future directions," *IEEE Wirel. Commun.*, vol. 31, no. 3, pp. 117–124, 2024.
[5] M. A. Albreem, M. Juntti, and S. Shahabuddin, "Massive MIMO detection techniques: A survey," *IEEE Commun. Surveys Tuts.*, vol. 21, no. 4, pp. 3109–3132, 2019.
[6] E. Björnson, Y. C. Eldar, E. G. Larsson, A. Lozano, and H. V. Poor, "Twenty-five years of signal processing advances for multiantenna communications: From theory to mainstream technology," *IEEE Signal Process. Mag.*, vol. 40, no. 4, pp. 107–117, 2023.
[7] S. Yang and L. Hanzo, "Fifty years of MIMO detection: The road to large-scale MIMOs," *IEEE Commun. Surveys Tuts.*, vol. 17, no. 4, pp. 1941–1988, 2015.
[8] D. Zhu, B. Li, and P. Liang, "On the matrix inversion approximation based on neumann series in massive MIMO systems," in *2015 IEEE Int. Conf. Commun. (ICC)*, pp. 1763–1769, IEEE, 2015.
[9] K. Izadinasab, A. W. Shaban, and O. Damen, "Low-complexity detectors for uplink massive MIMO systems leveraging truncated polynomial expansion," *IEEE Access*, vol. 10, pp. 91610–91621, 2022.
[10] L. Dai, X. Gao, X. Su, S. Han, C.-L. I, and Z. Wang, "Low-complexity soft-output signal detection based on gauss–seidel method for uplink multiuser large-scale MIMO systems," *IEEE Trans. Veh. Technol.*, vol. 64, no. 10, pp. 4839–4845, 2015.
[11] X. Gao, L. Dai, Y. Hu, Z. Wang, and Z. Wang, "Matrix inversion-less signal detection using sor method for uplink large-scale MIMO systems," in *2014 IEEE Global Commun. Conf.*, pp. 3291–3295, 2014.
[12] B. Kang, J.-H. Yoon, and J. Park, "Low-complexity massive MIMO detectors based on richardson method," *ETRI Journal*, vol. 39, no. 3, pp. 326–335, 2017.
[13] L. Li and J. Hu, "Fast-converging and low-complexity linear massive MIMO detection with L-BFGS method," *IEEE Trans. Veh. Technol.*, vol. 71, no. 10, pp. 10656–10665, 2022.
[14] L. Wei, C. Huang, G. C. Alexandropoulos, W. E. I. Sha, Z. Zhang, M. Debbah, and C. Yuen, "Multi-user holographic MIMO surfaces: Channel modeling and spectral efficiency analysis," *IEEE J. Sel. Topics Signal Process.*, vol. 16, no. 5, pp. 1112–1124, 2022.
[15] S. Berra, A. Benchabane, S. Chakraborty, K. Maruta, R. Dinis, and M. Beko, "A low complexity linear precoding method for extremely large-scale MIMO systems," *IEEE Open J. Veh. Technol.*, vol. 6, pp. 240–255, 2025.
[16] J. Liu, Y. Ma, J. Wang, and R. Tafazolli, "Accelerating iteratively linear detectors in multi-user (ELAA-)MIMO systems with UW-SVD," *IEEE Trans. Wireless Commun.*, vol. 23, no. 11, pp. 16711–16724, 2024.
[17] M. A. Albreem, W. Salah, A. Kumar, M. H. Alsharif, A. H. Rambe, M. Jusoh, and A. N. Uwaechia, "Low complexity linear detectors for massive MIMO: A comparative study," *IEEE Access*, vol. 9, pp. 45740–45753, 2021.
[18] M. W. Mahoney *et al.*, "Randomized algorithms for matrices and data," *Foundations and Trends® in Machine Learning*, vol. 3, no. 2, pp. 123–224, 2011.
[19] V. Bharadwaj, O. A. Malik, R. Murray, L. Grigori, A. Buluc, and J. Demmel, "Fast exact leverage score sampling from khatri-rao products with applications to tensor decomposition," *Advances Neural Inf. Process. Syst.*, vol. 36, 2024.
[20] T. G. Kolda and B. W. Bader, "Tensor decompositions and applications," *SIAM review*, vol. 51, no. 3, pp. 455–500, 2009.
[21] D. P. Woodruff *et al.*, "Sketching as a tool for numerical linear algebra," *Foundations and Trends® in Theoretical Computer Science*, vol. 10, no. 1–2, pp. 1–157, 2014.
[22] M. Dereziński and M. K. Warmuth, "Reverse iterative volume sampling for linear regression," *J. Mach. Learn. Res.*, vol. 19, no. 23, pp. 1–39, 2018.
[23] M. Derezinski, M. K. Warmuth, and D. J. Hsu, "Leveraged volume sampling for linear regression," *Advances Neural Inf. Process. Syst.*, vol. 31, 2018.
[24] M. Fahrbach, G. Fu, and M. Ghadiri, "Subquadratic kronecker regression with applications to tensor decomposition," *Advances Neural Inf. Process. Syst.*, vol. 35, pp. 28776–28789, 2022.
[25] T. H. Cormen, C. E. Leiserson, R. L. Rivest, and C. Stein, *Introduction to algorithms*. MIT press, 2022.